

Nonlinear Control of an AC-connected DC MicroGrid

A. Iovine^a, S. B. Siad^b, G. Damm^b, E. De Santis^a, M. D. Di Benedetto^a

Abstract—New connection constraints for the power network (Grid Codes) require more flexible and reliable systems, with robust solutions to cope with uncertainties and intermittence from renewable energy sources (renewables), such as photovoltaic arrays. A solution for interconnecting such renewables to the main grid is to use storage systems and a Direct Current (DC) MicroGrid. A "Plug and Play" approach based on the "System of Systems" philosophy using distributed control methodologies is developed in the present work. This approach allows to interconnect a number of elements to a DC MicroGrid as power sources like photovoltaic arrays, storage systems in different time scales like batteries and supercapacitors, and loads like electric vehicles and the main AC grid. The proposed scheme can easily be scalable to a much larger number of elements.

Keywords—DC/AC MicroGrid, Power generation control, Lyapunov methods, Grid stability

I. INTRODUCTION

Renewable energy is the key for locally producing clean and inexhaustible energy to supply the world's increasing demand for electricity. Photovoltaic (PV) conversion of solar energy is a promising way to meet the growing demand for energy, and is the best fit in several situations [1]. However, its intermittent nature remains a real disability that can create voltage (or even frequency in the case of islanded MicroGrids) instability for large scale grids. In order to answer to the new constraints of connection to the network (Grid Codes) it is possible to consider storage devices [2], [3]; the whole system will be able to inject the electric power generated by photovoltaic panels (or other renewables) to the grid in a controlled and efficient way. As a consequence, it is necessary to develop a strategy for managing energy in relation to the load and the storages' constraints. Direct Current (DC) microgrids are attracting interest thanks to their ability to easily integrate modern loads, renewable sources and energy storages [4], [5], [6], [7] since most of them (like electric vehicles, batteries and photovoltaic panels) are naturally DC: therefore, in this paper a DC microgrid composed by a source, a load, two storages working in different time scales, and their connecting devices is considered. These microgrids need to interact with the already existing infrastructure, that is an Alternate Current (AC) grid: in this work connection of the DC microgrid with a main AC grid is described, and the dedicated interconnecting power device is considered.

The utilized approach is based on a "Plug and Play" philosophy: the global control will be carried out at local level

by each actuator, according to distributed control paradigm. The controller is developed in a distributed way for stabilizing each part of the whole system, while performing power management in real time to satisfy the production objectives and assuring the stability of the interconnection to the main grid.

Control techniques for converters are a well known research field [8], [9], [10]: nevertheless, it is common practice to consider the hypothesis to have full controllability of the system [11], [12] while in reality, due to technical reasons, this will probably not be true. For example, realistic DC/DC converters have an additional variable (a capacitor) on the source side [13]. When this capacitor is controlled, another one (the grid side capacitor) is left uncontrolled. As explained in [14], this remaining dynamics is usually neglected by the assumption that it is connected (and implicitly stabilized) by an always stable strong main grid. Removing this assumption to consider a realistic grid implies that this dynamics needs to be taken into account when studying grid stability. In [14] the authors provide a rigorous stability analysis for a realistic DC MicroGrid. This work regards the connection of the aforementioned DC grid to an AC one, evaluating dynamics interaction when fulfilling request of a desired amount of active and reactive power from the AC grid. Stability conditions are evaluated for the interconnected case.

The adopted control strategy is shown to work both in islanded mode than in grid-connected mode: the AC grid is seen as a controllable load, while the load directly connected to the DC grid is uncontrolled (it can be constant or time-varying, both problems are relevant [15], [16]).

This paper is organized as follows. In Section II the model of the AC connected DC MicroGrid is introduced. Then in Section III the adopted control laws are introduced and stability requirements are proven to be satisfied. Section IV provides simulation results, while in Section V conclusions are offered.

II. MICROGRID

The reference framework is depicted in Figure 1, where the DC microgrid connected to the main AC is represented. The targets would be to assure voltage stability in the DC grid while correctly feeding power to the load; if possible, power is also provided to the main grid regulating both active and reactive power. To each component of the microgrid (PV array, battery, supercapacitor) a DC/DC converter is connected: their dynamical models are described in the following, as well as the AC/DC converter that connects the DC grid to the AC one.

The whole control objective is split in several tasks; the first one is to extract the maximum available power from the photovoltaic array. This maximum power production is obtained calculating the duty cycle in order to fix the voltage

^a Alessio Iovine, Elena De Santis and Marika Di Benedetto are with the Center of Excellence DEWS, Department of Information Engineering, Computer Science and Mathematics, University of L'Aquila, Italy. Email: alessio.iovine@graduate.univaq.it, {elena.desantis, mariadomenica.dibenedetto}@univaq.it.

^b Sabah B. Siad and Gilney Damm are with IBISC - Université d'Evry Val d'Essonne, Evry, France. Email: gilney.damm@ibisc.fr, siadsabah@yahoo.fr. This work is partially supported iCODE project.

of the capacitor directly connected to the PV array to a given reference.

The focus then moves to the storage systems and their connection to the DC network. In this paper, two kinds of storage are considered: a battery, which purpose is to provide/absorb the power when needed, and a supercapacitor, which purpose is to stabilize the DC grid voltage in case of disturbances. DC/DC bidirectional converters are necessary to enable the two modes of functioning (charge and discharge). The battery is assimilated as a reservoir which acts as a buffer between the flow requested by the network and the flow supplied by the production sources, and its voltage is controlled by the DC/DC current converter. With this structure, the DC grid is able to provide a continuous supply of good quality energy. The model introduced in [17] is here used for the supercapacitor.

Considering the availability of power, it can be provided to the main AC grid. An AC/DC converter is dedicated to manage the interconnection of the two grids; its purpose is to provide a desired amount of power to the AC grid, regulating both active and reactive power.

The converters present in this system must, in a distributed way, keep the stability of the mixed DC/AC network interconnecting all parts. The final management system can be configurable and adaptable as needed.

A. Assumptions

In this paper two main assumptions are made: the first one is the existence of a higher level controller which provide references to be accomplished by the local controllers [18]; the second one is about a proper sizing of each component of the microgrid in order to have feasible power balance.

Assumption 1: A higher level controller provides references for the local controllers: these references change every fixed time interval T and concern the amount of power needed for the next time interval and the desired voltage value for the DC grid. The time interval T is decided by the high level controller according to the computational time needed for calculations. These references are about the desired voltage to impose to the PV array and to the battery to obtain the needed amount of power, V_1^* and V_4^* respectively, the desired voltage value for the DC grid, V_9^* , and the desired currents to have a proper amount of active and reactive power to provide to the AC grid, I_d^* and I_q^* . The references must be able to take into account a proper charge/discharge rate power for the supercapacitor.

Assumption 2: The sizing of the photovoltaic array is performed according to total energy needed into a whole day, and the sizing of the battery and the supercapacitor are performed according to the energy balance in a T time step, needed for selecting a new reference.

B. Grid modeling

Here the circuital representation and the mathematical models are given, based on power electronics averaging technique for the DC/DC converters [19], [20], while the model for the AC/DC converter is given by [21], [22].

The resulting DC MicroGrid system is the composition of circuits in Figure 1, generating the model introduced in the

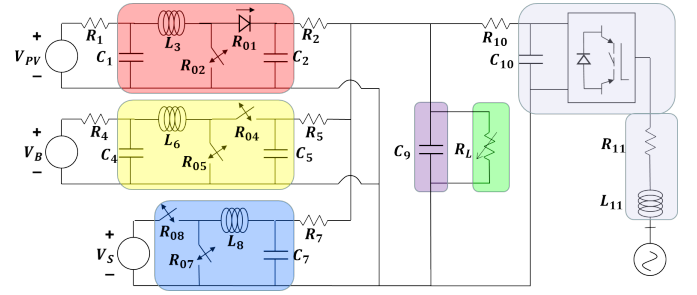


Figure 1. The considered framework: the red area describes the DC/DC boost converter connected to the PV array, while the yellow one the DC/DC bidirectional one connected to the battery. The DC/DC buck converter connecting the supercapacitor is in the blue area, while the AC/DC converter connecting the DC grid to the AC one is in the grey area. The uncontrollable load is in the green area, while the capacitor representing the DC grid in the violet one.

following:

$$x = \begin{bmatrix} x_1 \\ x_2 \\ x_3 \\ x_4 \\ x_5 \\ x_6 \\ x_7 \\ x_8 \\ x_9 \\ x_{10} \\ x_{11} \\ x_{12} \end{bmatrix} = \begin{bmatrix} C_1 \text{ capacitor voltage} \\ C_2 \text{ capacitor voltage} \\ L_3 \text{ inductor current} \\ C_4 \text{ capacitor voltage} \\ C_5 \text{ capacitor voltage} \\ L_6 \text{ inductor current} \\ C_7 \text{ capacitor voltage} \\ L_8 \text{ capacitor voltage} \\ C_9 \text{ capacitor voltage} \\ C_{10} \text{ capacitor voltage} \\ L_{11} \text{ inductor current } i_d \\ L_{11} \text{ inductor current } i_q \end{bmatrix} \quad (1)$$

$$\begin{cases} \dot{x}_1 = -\frac{1}{R_1 C_1} x_1 - \frac{1}{C_1} x_3 + \frac{1}{R_1 C_1} V_{PV} \\ \dot{x}_2 = -\frac{1}{R_2 C_2} x_2 + \frac{1}{C_2} x_3 - \frac{1}{C_2} u_1 x_3 + \frac{1}{R_2 C_2} x_9 \\ \dot{x}_3 = \frac{1}{L_3} x_1 - \frac{1}{L_3} x_2 - \frac{R_{01}}{L_3} x_3 + \frac{1}{L_3} x_2 u_1 + \frac{R_{01} - R_{02}}{L_3} x_3 u_1 \\ \dot{x}_4 = -\frac{1}{R_4 C_4} x_4 - \frac{1}{C_4} x_6 + \frac{1}{R_4 C_4} V_B \\ \dot{x}_5 = -\frac{1}{R_5 C_5} x_5 + \frac{1}{C_5} x_6 - \frac{1}{C_5} u_2 x_6 + \frac{1}{R_5 C_5} x_9 \\ \dot{x}_6 = \frac{1}{L_6} x_4 - \frac{1}{L_6} x_5 - \frac{R_{04}}{L_6} x_6 + \frac{1}{L_6} x_5 u_2 \\ \dot{x}_7 = -\frac{1}{R_7 C_7} x_7 - \frac{1}{C_7} x_8 + \frac{1}{R_7 C_7} x_9 \\ \dot{x}_8 = \frac{1}{L_8} V_S u_3 - \frac{R_{08}}{L_8} x_8 - \frac{1}{L_8} x_7 \\ \dot{x}_9 = \frac{1}{C_9} \left(\frac{1}{R_2} (x_2 - x_9) + \frac{1}{R_5} (x_5 - x_9) \right) + \\ + \frac{1}{C_9} \left(\frac{1}{R_7} (x_7 - x_9) + \frac{1}{R_{10}} (x_{10} - x_9) - \frac{1}{R_L} x_9 \right) \\ \dot{x}_{10} = -\frac{3}{2 C_{10}} \frac{1}{x_{10}} (v_{ld} x_{11} + v_{lq} x_{12}) + \frac{1}{R_{10} C_{10}} (x_9 - x_{10}) \\ \dot{x}_{11} = \frac{1}{L_{11}} [-R_{11} x_{11} + \omega x_{12} + \frac{1}{2} x_{10} u_4 - v_{ld}] \\ \dot{x}_{12} = \frac{1}{L_{11}} [-R_{11} x_{12} - \omega x_{13} + \frac{1}{2} x_{10} u_5 - v_{lq}] \end{cases} \quad (2)$$

$$\dot{x}(t) = f(x(t)) + g(x(t), u(t), d(t)) + d(t) \quad (3)$$

$$u = [u_1 \ u_2 \ u_3 \ u_4 \ u_5]^T \quad (4)$$

$$d = [V_{PV} \ V_B \ V_S \ R_L \ v_{ld} \ v_{lq} \ \omega]^T \quad (5)$$

where $C_1, C_2, C_4, C_5, C_7, C_9, C_{10}, R_1, R_2, R_{01}, R_{02}, R_4, R_5, R_{04}, R_{05}, R_7, R_{07}, R_{08}, R_{10}, R_{11}, R_L, L_3, L_6, L_8, L_{11}$, are known positive values of the capacitors, resistances and the inductor. $V_{PV} > 0, V_B > 0$ are constant positive values of the PV array and the battery voltages, while V_S is a slowing time varying positive value known at each time t representing the voltage of the supercapacitor. $v_{ld} \geq 0$ and $v_{lq} \geq 0$ are the AC relative voltages, while ω is the frequency of the AC grid. The control inputs in u are the duty cycles of the converters.

We can now refer the references to the state variables: the voltage value V_1^* to impose the maximum power tracking provides a reference x_1^* for dynamics x_1 , while V_4^* and V_9^* refer to x_4^* and x_9^* . The references I_d^* and I_q^* (relative to the desired active and reactive powers provided to the AC grid) for the currents are related to the dynamics x_{11} and x_{12} , x_{11}^* and x_{12}^* respectively.

III. CONTROLLERS

Considering the hypothesis in Section II-A, given the constant values of the resistance R_L , voltages x_1^* and x_4^* that allow power balance in steady-state with respect to the demanded currents x_{11}^* and x_{12}^* at the desired voltage grid x_9^* , it is possible to state that:

Theorem 1: Control inputs u_1, u_2, u_3, u_4, u_5 exist such that the system in (2) is asymptotically stable in closed loop around the equilibrium point x^e ;

$$x^e = \begin{bmatrix} x_1^e \\ x_2^e \\ x_3^e \\ x_4^e \\ x_5^e \\ x_6^e \\ x_7^e \\ x_8^e \\ x_9^e \\ x_{10}^e \\ x_{11}^e \\ x_{12}^e \end{bmatrix} = \begin{bmatrix} x_1^* \\ x_2^* \\ \frac{1}{R_1}(V_{PV} - x_1^*) \\ x_4^* \\ x_5^* \\ \frac{1}{R_4}(V_B - x_4^*) \\ x_9^* \\ 0 \\ x_9^* \\ x_{10}^* \\ x_{11}^* \\ x_{12}^* \end{bmatrix} \quad (6)$$

Proof: The proof is based on a composition of Lyapunov functions, a methodology described in [23]. Indeed the control inputs

$$u_1 = \frac{1}{x_2 + (R_{01} - R_{02})x_3} [-x_1 + x_2 + R_{01}x_3 - L_3v_1] \quad (7)$$

$$u_2 = \frac{1}{x_5} (-x_4 + x_5 + R_{04}x_6 + L_6v_2) \quad (8)$$

$$u_4 = 2\frac{1}{x_{10}} [v_{ld} + R_{11}x_{11} - \omega x_{12} - L_{11}v_4] \quad (9)$$

$$u_5 = 2\frac{1}{x_{10}} [v_{lq} + R_{11}x_{12} + \omega x_{11} - L_{11}v_5] \quad (10)$$

with

$$v_1 = K_3(x_3 - z_3) + \bar{K}_3\alpha_3 - C_1\bar{K}_1K_1^\alpha(x_1 - x_1^*) + \left(C_1K_1 - \frac{1}{R_1}\right)(K_1(x_1 - x_1^*) + \bar{K}_1\alpha_1) \quad (11)$$

$$z_3 = \frac{1}{R_1}(V_{PV} - x_1) + C_1K_1(x_1 - x_1^*) + C_1\bar{K}_1\alpha_1 \quad (12)$$

$$\dot{\alpha}_1 = K_1^\alpha(x_1 - x_1^*) \quad \dot{\alpha}_3 = K_3^\alpha(x_3 - z_3) \quad (13)$$

$$v_2 = -K_6(x_6 - z_6) - \bar{K}_6\alpha_6 + \bar{K}_4K_4^\alpha(x_4 - x_4^*) + \left(C_4K_4 - \frac{1}{R_4}\right)(K_4(x_4 - x_4^*) + \bar{K}_4\alpha_4) \quad (14)$$

$$z_6 = \left(\frac{1}{R_4}(V_B - x_4) + C_4K_4(x_4 - x_4^*) + C_4\bar{K}_4\alpha_4\right) \quad (15)$$

$$\dot{\alpha}_4 = K_4^\alpha(x_4 - x_4^*) \quad \dot{\alpha}_6 = K_6^\alpha(x_6 - z_6) \quad (16)$$

$$v_4 = K_{11}(x_{11} - x_{11}^*) + \bar{K}_{11}\alpha_{11} \quad (17)$$

$$v_5 = K_{12}(x_{12} - x_{12}^*) + \bar{K}_{12}\alpha_{12} \quad (18)$$

$$\dot{\alpha}_{11} = K_{11}^\alpha(x_{11} - x_{11}^*) \quad \dot{\alpha}_{12} = K_{12}^\alpha(x_{12} - x_{12}^*) \quad (19)$$

where the $\alpha_i, i = 1, 3, 4, 6, 11, 12$, are integral terms assuring zero error in steady state and the positive gains $K_i, \bar{K}_i, K_i^\alpha, i = 1, 3, 4, 6, 11, 12$, are properly chosen, provide a Proportional Integral (PI) control action that feedback linearizes the dynamics $x_i, i = 1, 3, 4, 6, 11, 12$, providing asymptotic stability. Then it is possible to calculate positive definite Lyapunov functions $V_{1,3}, V_{4,6}, V_{11,12}$, such that their time derivative are negative definite. The Lyapunov function for the entire system is therefore selected as

$$V = V_{1,3} + V_{4,6} + V_{11,12} + V_{2,5,9,10} + V_{7,8} \quad (20)$$

where $V_{7,8}$ and $V_{2,5,9,10}$ need to be described. We start from the last one, that describes the interconnection among the subsystems:

$$V_{2,5,9,10} = \frac{C_2}{2}(x_2 - x_2^*)^2 + \frac{C_5}{2}(x_5 - x_5^*)^2 + \frac{C_{10}}{2}(x_{10} - x_{10}^*)^2 + \frac{C_9}{2}x_9^2 \quad (21)$$

According to the calculation of its time derivative, the dynamics x_7 can be used as control variable to obtain a negative semidefinite derivative; indeed, we can properly select a reference z_7 for x_7 such that

$$\dot{V}_{2,5,9,10} = -\frac{1}{R_2}(x_2 - x_2^*)^2 - \frac{1}{R_5}(x_5 - x_5^*)^2 + \left(-\frac{1}{R_{10}}(x_{10} - x_{10}^*)^2 - \frac{1}{R_7}(x_9 - x_9^*)^2\right) \leq 0 \quad (22)$$

To prove asymptotic stability the set Ω is considered: it is the largest invariant set of the set E of all points where the Lyapunov function is not decreasing. Ω contains an unique point; then applying LaSalle's theorem, asymptotic stability of the equilibrium point can be established.

$$\Omega = \{(x_2, x_5, x_{10}, x_9) : x_2 = x_2^*, x_5 = x_5^*, x_{10} = x_{10}^*, x_9 = x_9^*\} = \{(x_2^*, x_5^*, x_{10}^*, x_9^*)\} \quad (23)$$

To impose the reference z_7 backstepping technique is used: a reference z_8 for the dynamics x_8 is selected in order to force the dynamics of x_7 to track the reference z_7 , and a proper control law u_3 is calculated for the convergence of x_8 to z_8 . The following Lyapunov function can be used to determine the control law:

$$V_{7,8} = \frac{1}{2}(x_7 - z_7)^2 + \frac{1}{2}(x_8 - z_8)^2 \quad (24)$$

where $K_7 > 0, K_8 > 0$,

$$z_8 = \frac{1}{R_7}(x_9 - x_7) + C_7K_7(x_7 - z_7) - C_7\dot{z}_7 \quad (25)$$

With the control law defined in the following

$$u_3 = \frac{1}{V_S} [x_7 + R_{08}x_8 + L_8\dot{z}_8 - L_8v_3] \quad (26)$$

where

$$v_3 = K_8(x_8 - z_8) \quad (27)$$

$$\dot{z}_8 = \frac{1}{R_7}\dot{x}_9 - C_7K_7\dot{z}_7 - K_7\left(K_7C_7 - \frac{1}{R_7}\right)(x_7 - z_7) - C_7\ddot{z}_7 \quad (28)$$

the considered Lyapunov function in (24) has a negative definite time derivative:

$$\dot{V}_{7,8} = -K_7(x_7 - z_7)^2 - K_8(x_8 - z_8)^2 \quad (29)$$

Then the Lyapunov function V in (20) has the following time derivative that ensures asymptotic stability:

$$\dot{V} = \dot{V}_{1,3} + \dot{V}_{4,6} + \dot{V}_{11,12} + \dot{V}_{7,8} + \dot{V}_{2,5,9,10} \leq 0 \quad (30)$$

Remark 1: In accordance to the equilibria in (6), the power balance requirement is satisfied. The value of z_7 in steady-state can be written as

$$\frac{x_7^*}{R_7} = \frac{x_9^*}{R_L} - \frac{1}{R_2}(x_2^* - x_9^*) - \frac{1}{R_5}(x_5^* - x_9^*) - \frac{1}{R_{10}}(x_{10}^* - x_9^*) + \frac{x_9^*}{R_7} \quad (31)$$

where the values of x_2^* , x_5^* and x_{10}^* depends on the given equilibrium values and on the control inputs. At the equilibrium, the following condition is satisfied:

$$\frac{x_9^*}{R_L} = \frac{1}{R_2}(x_2^* - x_9^*) + \frac{1}{R_5}(x_5^* - x_9^*) + \frac{1}{R_{10}}(x_{10}^* - x_9^*) \quad (32)$$

Condition (32) describes the power balance when all the "bricks" fit their target to provide/take the right amount of power; implicitly, it can be stated that $x_7^* = x_9^*$.

Theorem 1 refers to an unconstrained problem: due to the physics of the devices and of the meaning of the controllers, all the control inputs are bounded. The bounds we must consider are: $u_1 \in [0, 1]$, $u_2 \in [0, 1]$, $u_3 \in [0, 1]$, $\sqrt{u_4^2 + u_5^2} \leq 1$ (see [8], [9]).

The domain of operation for the state variables is restricted (e.g. $x_9 \in [x_9^m, x_9^M]$, where $x_9^m \geq \max(V_{PV}, V_B)$ and $x_9^M \leq V_S$). However in [14] we proved that the set of initial states such that the above defined input constraints are satisfied, for any evolution of the controlled system, contains the equilibrium in its interior.

IV. SIMULATIONS

In this section we present some simulations that show the results obtained using the proposed control inputs. Matlab has been used for obtaining such simulations. The values of the parameters are depicted in Tables I.

The simulation target is to correctly feed a load while maintaining the grid stability, which means to ensure no large variation in the DC grid voltage. The load is composed by an uncontrollable part, which is a resistance, and a controllable one, which is the AC grid. The simulation time is twenty seconds. The fixed value x_9^* for the DC grid voltage is selected

Table I
GRID PARAMETERS.

Parameter	Value	Parameter	Value
C_1	100 mF	L_3	33 mH
C_2	10 mF	R_{01}	10 mΩ
R_1	100 mΩ	R_{02}	10 mΩ
R_2	100 mΩ	C_4	100 mF
C_5	10 mF	R_{04}	10 mΩ
R_4	100 mΩ	R_{05}	10 mΩ
R_5	10 mΩ	L_6	33 mH
C_7	10 mF	L_8	3.3 mH
R_{07}	10 mΩ	R_{08}	10 mΩ
R_7	100 mΩ	C_9	0.1 mF
R_{10}	100 mΩ	L_{11}	3.3 mH
R_{11}	10 mΩ	C_{10}	680 μF
f	50 Hz		

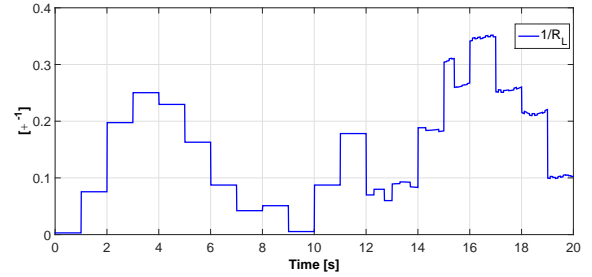


Figure 2. The load conductance $\frac{1}{R_L}$.

as $x_9^* = 1000$ V. The secondary controller provides the references to be reached each time interval (1 second); during that period the introduced control laws bring the devices to operate in the desired points. Figure 2 depicts the uncontrollable load; it is possible to see its piecewise constant behavior until the simulation time of twelve seconds, when it starts to be time-varying. Figure 3 describes the currents related to the power demanded by the AC grid; the current related to reactive power is always kept to zero reference, while the active one is demanded in a time window of eleven seconds after three seconds. The choice to send zero reactive power is due to the fact that the remuneration of power production is solely based on active power; selection of providing both of them is feasible if needed, and is the case when fully controlling frequency and voltage of the AC MicroGrid.

The considered simulation framework contains different situations: as we have already seen, the load has step variations and a time varying part. Furthermore, disturbances acting on the PV voltage are considered (see Figure 4). Moreover, the

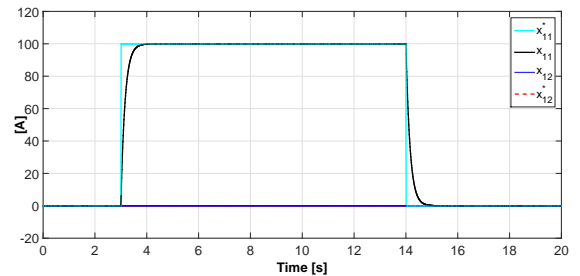


Figure 3. The currents in the inductance L_{11} following their references: the current related to the active power (x_{11}) is the black line, tracking its cyan reference, while the one related to the reactive power (x_{12}) is depicted by the blue line which is tracking the red line representing its reference.

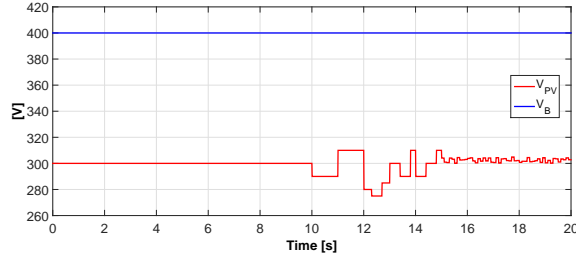


Figure 4. The voltages of V_{PV} (red line) and V_B (blue line).

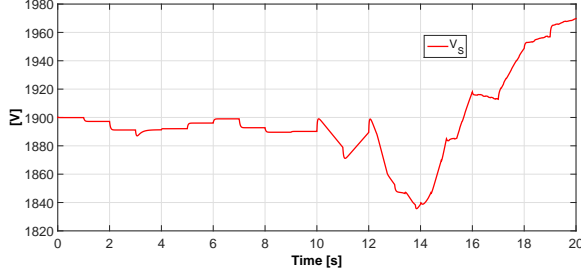


Figure 5. The voltage of the supercapacitor.

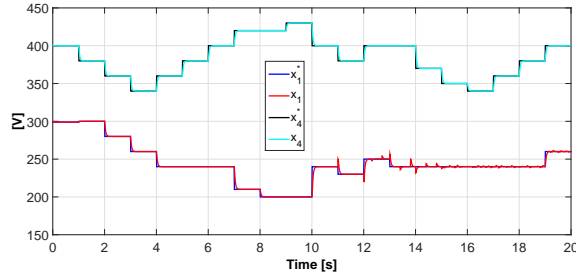


Figure 6. The voltages of C_1 (red line) and C_4 (cyan line) following the desired references, the blue and black lines, respectively.

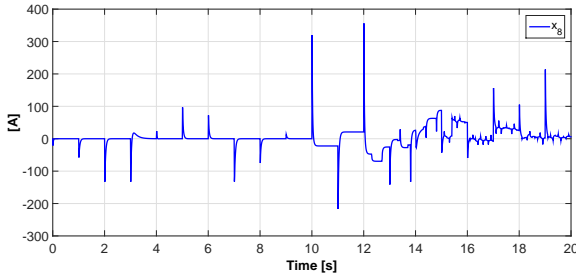


Figure 7. The current in the inductance L_8 .

case where the references do not fulfill the energy balance without the power provided by the supercapacitor is considered: there the supercapacitor will need to provide power during all the time window, and its reservoir will change over the time, as depicted in Figure 5. Here we considered the voltage of the battery not to be affected by the current behavior; indeed a constant value is used to represent it because the battery is supposed to be sized in such a way that it is not affected by current dynamics over a time of twenty seconds. The resulting current generated by the supercapacitor is then introduced in Figure 7; it is mainly due to the necessity of the supercapacitor to ensure DC grid voltage stability around the equilibrium value of x_9^* when there is a mismatch due to the transient or disturbances, but in the second half

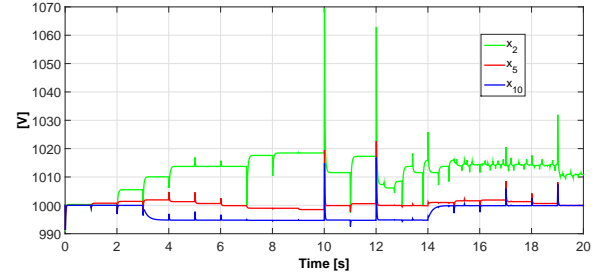


Figure 8. The voltages of C_2 (green line), C_5 (red line) and C_{10} (blue line).

of the simulation it is also providing the power needed to compensate power mismatch due to wrong reference choice by the higher level controller. Indeed, in accordance to the values of the load, the references x_1^* and x_4^* are obtained for the power balance target; if they are not sized for the power demand, the supercapacitor has also the described role.

As depicted in Figure 6, the C_1 and C_4 capacitor voltages reach the desired values during the considered time step. Two different situations for the controllers are faced because the devices need two different treatments; we need from the PV array to start providing the highest level of power as soon as possible, while the battery needs to have a smooth behavior to preserve its life-time. The resulting voltage dynamics on the grid connected capacitors C_2 , C_5 , C_{10} , are modified by the current flow generated by the sources; all the dynamics are stable, as shown in Figure 8. Their evolution is influenced by the value of the DC grid voltage, which is the capacitor C_9 ; its value over time is depicted in Figure 9. To satisfy stability constraints, in response to the load variations and to the missing power coming from the PV and the battery, the voltage of the capacitor C_7 reacts balancing the energy variation. It is possible to verify that the worst spikes correspond to a very high variations in the grid dynamics, but nevertheless they are less than 10% of the values.

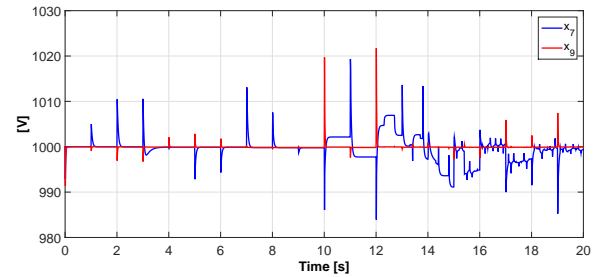


Figure 9. The voltages of C_7 (blue line) and C_9 (red line).

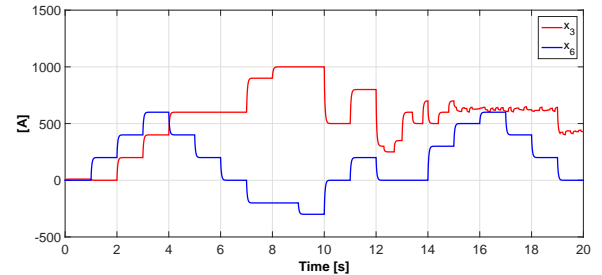


Figure 10. The currents in the inductances L_3 (red line) and L_6 (blue line).

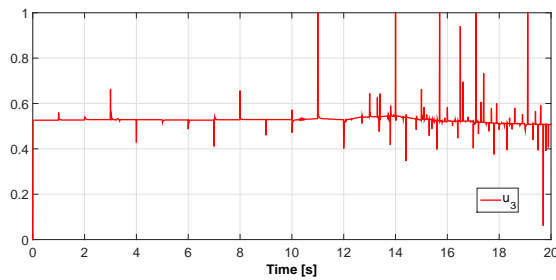


Figure 11. The control input u_3 .

Figure 10 describes the current coming from the PV and the one related to the charge/discharge mode of the battery: these dynamics are dependent on the voltages and related to them. The control input for the DC/DC converter connected to the supercapacitor is depicted in Figure 11: its variation depends on the variations of voltage V_S (see Figure 5) and of the load (see Figures 3 and 7).

Finally, we can state that the desired target to maintain DC grid voltage stability while providing a certain amount of power to a load composed by a controllable part and an uncontrollable one is ensured with the proposed control laws. The simulation describe result validity in a range of situations.

V. CONCLUSIONS

In this paper the connection of a DC microgrid with the main AC grid is addressed. A DC grid composed by a renewable source and two kinds of storages, acting as energy and power reservoirs, is considered to solve the problem of correctly feeding a load; such load is composed by an uncontrollable part and a controllable one, which is the power provided to the AC grid. The modeling of the resulting grid composed by the dedicated connected devices is presented and control laws are obtained to properly satisfy requirements of voltage stability and power balance. Formal conditions are introduced to describe the problem and rigorous analysis are carried out to obtain stability results. Simulations show that the proposed control action successfully fits the desired target to feed the load while keeping the voltage of the DC grid at a desired value.

REFERENCES

- [1] M. A. Eltawil and Z. Zhao, "Grid-connected photovoltaic power systems: Technical and potential problems. A review," *Renewable and Sustainable Energy Reviews*, vol. 14, no. 1, pp. 112 – 129, 2010.
- [2] J. Barton and D. Infield, "Energy storage and its use with intermittent renewable energy," *Energy Conversion, IEEE Transactions on*, vol. 19, pp. 441–448, June 2004.
- [3] G. Krajai, N. Dui, Z. Zmijarevi, B. V. Mathiesen, A. A. Vuini, and M. da Graa Carvalho, "Planning for a 100% independent energy system based on smart energy storage for integration of renewables and CO₂ emissions reduction," *Applied Thermal Engineering*, vol. 31, no. 13, pp. 2073 – 2083, 2011.
- [4] P. Piagi and R. Lasseter, "Autonomous control of microgrids," in *Power Engineering Society General Meeting, 2006. IEEE*, pp. 8 pp.–, 2006.
- [5] N. Hatziaegyriou, H. Asano, R. Iravani, and C. Marnay, "Microgrids," *Power and Energy Magazine, IEEE*, vol. 5, pp. 78–94, July 2007.
- [6] T. Dragicevic, J. Vasquez, J. Guerrero, and D. Skrlac, "Advanced LVDC Electrical Power Architectures and Microgrids: A step toward a new generation of power distribution networks," *Electrification Magazine, IEEE*, vol. 2, pp. 54–65, March 2014.
- [7] J. Guerrero, P. C. Loh, T.-L. Lee, and M. Chandorkar, "Advanced Control Architectures for Intelligent Microgrids Part II: Power Quality, Energy Storage, and AC/DC Microgrids," *Industrial Electronics, IEEE Transactions on*, vol. 60, pp. 1263–1270, April 2013.

- [8] H. J. Sira Ramirez and R. Silva-Ortigoza, *Control design techniques in power electronics devices*. Springer, 2006.
- [9] Y. Chen, G. Damm, A. Benchaib, and F. Lamnabhi-Lagarigue, "Multi-time-scale stability analysis and design conditions of a VSC terminal with DC voltage droop control for HVDC networks," in *53rd IEEE Conference on Decision and Control*, pp. 3266–3271, Dec 2014.
- [10] Y. Chen, G. Damm, A. Benchaib, M. Netto, and F. Lamnabhi-Lagarigue, "Control induced explicit time-scale separation to attain DC voltage stability for a VSC-HVDC terminal," in *19th IFAC World Congress on International Federation of Automatic Control (IFAC 2014)*, vol. 19, (Cape Town, South Africa), pp. 540–545, Aug. 2014.
- [11] A. P. N. Tahim, D. J. Pagano, E. Lenz, and V. Stramosk, "Modeling and stability analysis of islanded dc microgrids under droop control," *IEEE Transactions on Power Electronics*, vol. 30, no. 8, pp. 4597–4607, 2015.
- [12] A. Bidram, A. Davoudi, F. L. Lewis, and J. M. Guerrero, "Distributed Cooperative Secondary Control of Microgrids Using Feedback Linearization," *IEEE Transactions on Power Systems*, vol. 28, no. 3, pp. 3462–3470, 2013.
- [13] G. Walker and P. Sernia, "Cascaded DC-DC converter connection of photovoltaic modules," *Power Electronics, IEEE Transactions on*, vol. 19, pp. 1130–1139, July 2004.
- [14] A. Iovine, G. Damm, E. De Santis, M. D. Di Benedetto, A. Benchaib, and S. B. Siad, "Nonlinear control of a DC microgrid for the integration of photovoltaic panels," *Submitted, draft on arXiv <http://arxiv.org/abs/1608.00844>*.
- [15] D. Marx, P. Magne, B. Nahid-Mobarakeh, S. Pierfederici, and B. Davat, "Large Signal Stability Analysis Tools in DC Power Systems With Constant Power Loads and Variable Power Loads; A Review," *Power Electronics, IEEE Transactions on*, vol. 27, pp. 1773–1787, April 2012.
- [16] D. Hamache, A. Fayaz, E. Godoy, and C. Karimi, "Stabilization of a DC electrical network via backstepping approach," in *Industrial Electronics (ISIE), IEEE 23rd International Symposium on*, pp. 242–247, June 2014.
- [17] D. Lifshitz and G. Weiss, "Optimal control of a capacitor-type energy storage system," *Automatic Control, IEEE Transactions on*, vol. 60, pp. 216–220, Jan 2015.
- [18] D. Olivares, A. Mehrizi-Sani, A. Etemadi, C. Canizares, R. Iravani, M. Kazerani, A. Hajimiragha, O. Gomis-Bellmunt, M. Saeedifard, R. Palma-Behnke, G. Jimenez-Estevéz, and N. Hatziaegyriou, "Trends in microgrid control," *Smart Grid, IEEE Transactions on*, vol. 5, pp. 1905–1919, July 2014.
- [19] S. Sanders, J. Noworolski, X. Liu, and G. C. Verghese, "Generalized averaging method for power conversion circuits," *Power Electronics, IEEE Transactions on*, vol. 6, pp. 251–259, Apr 1991.
- [20] R. Middlebrook and S. Cuk, "A general unified approach to modelling switching-converter power stages," *International Journal of Electronics*, vol. 42, no. 6, pp. 521–550, 1977.
- [21] V. Blasko and V. Kaura, "A new mathematical model and control of a three-phase AC-DC voltage source converter," *Power Electronics, IEEE Transactions on*, vol. 12, pp. 116–123, Jan 1997.
- [22] E. Song, A. Lynch, and V. Dinavahi, "Experimental validation of nonlinear control for a voltage source converter," *Control Systems Technology, IEEE Transactions on*, vol. 17, pp. 1135–1144, Sept 2009.
- [23] P. Kundur, J. Paserba, V. Ajjarapu, G. Andersson, A. Bose, C. Canizares, N. Hatziaegyriou, D. Hill, A. Stankovic, C. Taylor, T. Van Cutsem, and V. Vittal, "Definition and classification of power system stability IEEE/CIGRE joint task force on stability terms and definitions," *Power Systems, IEEE Transactions on*, vol. 19, pp. 1387–1401, Aug 2004.